ELSEVIER

Journal of Organometallic Chemistry 540 (1997) 7–13

Journal of Organometallic Chemistry

Equilibrium constants and kinetics of carbon monoxide insertion in alkyl complexes of ruthenium(II)

Gianfranco Bellachioma, Giuseppe Cardaci *, Alceo Macchioni, Gustavo Reichenbach

Dipartimento di Chimica, Università di Perugia, I-06100 Perugia, Italy

Received 5 August 1996; revised 10 December 1996

Abstract

The equilibrium constants of the reaction of *cis, trans*-[$Ru(CO)_2(PMe_3)_2(CH_3)I$] (**Mc**) with carbon monoxide to give *cis, trans*-[$Ru(CO)_2(PMe_3)_2(COMe)I$] (**Ac**) and *trans, trans*-[$Ru(CO)_2(PMe_3)_2(COMe)I$] (**At**) were measured at various temperatures in toluene. The thermodynamic parameters are compared with those obtained for the isoelectronic complexes of iron, and the trend is discussed. The kinetics of the carbonylation reaction of **Mc**, as well as those of the inverse decarbonylation reaction of **At** were measured. The kinetics of the carbonylation of the new complex *trans, trans*-[$Ru(CO)_2(PMe_3)_2(CH_3)I$] (**Mt**) were also investigated. All the results afford further support to the previously proposed CO insertion mechanism occurring via methyl migration. The comparison of these kinetic results with those of isoelectronic complexes of iron indicates that ruthenium is more reactive than iron, which is reflected by its greater aptitude to act as catalyst in many processes. © 1997 Elsevier Science S.A.

Keywords: CO insertion; Ruthenium complexes; Mechanism; Equilibrium constants

1. Introduction

Carbon monoxide insertion in the metal–alkyl bond is one of the most important steps in homogeneous catalysis with organometallic complexes [1]. The kinetics [2], thermodynamics [3] and stereochemistry [4] of this reaction have been extensively studied. The reaction proceeds via migration of the alkyl group onto a *cis*-CO with the consequent creation of a vacant coordination position [5] that is usually occupied by an entering nucleophile. The effects of the ancillary ligands on the insertion reaction are explained on the basis of their influence on the metal–alkyl bond strength [6].

Surprisingly few studies have been carried out on the effect of the nature of the metal in isoelectronic series [7]. We undertook a study of this effect upon the isoelectronic [$M(CO)_2L_2RX$] complexes (M = Fe, Ru, Os; L = phosphine ligands; R = methyl and X = I). The results of a study on iron complexes have been published previously [8,9].

Ruthenium complexes *cis, trans*-[$Ru(CO)_2L_2RX$] react with carbon monoxide to initially give the acetyl complexes *cis, trans*-[$Ru(CO)_2L_2(COR)X$] which isomerizes to *trans, trans*-[$Ru(CO)_2L_2(COR)X$] [10,11]. The stereochemistry and the mechanism of this reaction have been clarified by a qualitative study of the reaction with nucleophiles [10] and by isotopic labelling with ^{13}CO [11]. The results exclude the previously proposed mechanism via CO migration [12], and confirm the methyl migration mechanism [2].

In this paper we present the results of a quantitative study of the kinetics and thermodynamics of the carbonylation reaction of *cis, trans*-[$Ru(CO)_2(PMe_3)_2(CH_3)I$] (**Mc**) and of the new complex *trans, trans*-[$Ru(CO)_2(PMe_3)_2(CH_3)I$] (**Mt**) (kinetics only) (see Scheme 1); these results are compared with those obtained for the isoelectronic iron complexes.

2. Experimental details

2.1. General

PMe_3 was prepared as described in Ref. [13]; *cis, trans*-[$Ru(CO)_2(PMe_3)_2MeI$] (**Mc**) was prepared as described in Ref. [14]; toluene and other solvents were purified by standard methods [15]. Since *cis, trans*-

* Corresponding author.

PII S0022-328X(97)00035-1

$[Ru(CO)_2(PMe_3)_2(COMe)I]$ (**Ac**) cannot be isolated due to its high isomerization rate, even at 0 °C, it was characterized spectroscopically: IR spectrum (*n*-hexane): ν_{CO} = 1980 (s), 2038 (s) cm^{-1}; ^1H NMR spectrum (CH_2Cl_2): δ_{COMe} = 2.34 (s) ppm; δ_{PMe_3} = 1.71 (t) ppm, $|^2J_{PH} + {}^4J_{PH}|$ = 3.8 Hz; ^{31}P NMR spectrum (CD_2Cl_2): δ_P = −16.9 (s) ppm. IR spectra were recorded on a 983 Perkin–Elmer dispersive spectrophotometer or on a 1725X FT-IR Perkin–Elmer spectrophotometer. ^1H and ^{31}P NMR spectra were recorded with an AC200 Bruker spectrometer. The ^1H chemical shifts were related to tetramethylsilane as internal reference and the ^{31}P chemical shifts were relative to 85% H_3PO_4 in D_2O as external reference with a positive sign indicating a shift to lower field.

2.2. Preparation of trans, trans-$[Ru(CO)_2(PMe_3)_2(COMe)I]$ (At)

Mc (2.5 g) was dissolved in *n*-hexane (50 ml). CO was bubbled in the solution at room temperature. After 30 min equilibrium was reached: **Mc**, **At** and **Ac** were present. Complex **At** was crystallized from this solution at −18 °C as a white crystalline solid: 2 g (yield 80%): anal. calcd: C, 25.03; H, 4.41; found: C, 25.28; H,4.61. IR spectrum (*n*-hexane). ν_{CO} = 1986 (vs), 2077 (vw) cm^{-1}; ^1H NMR spectrum (CD_2Cl_2): δ_{COMe} = 2.49 (s) ppm; δ_{PMe_3} = 1.61 (t) ppm, $|^2J_{PH} + {}^4J_{PH}|$ = 3.7 Hz; ^{31}P NMR (CD_2Cl_2): δ_P = −14.6 (s) ppm.

2.3. Preparation of trans, trans-$[Ru(CO)_2(PMe_3)_2MeI]$ (Mt)

Finely powdered crystals of **Mc** (2 g) were irradiated in a glass vessel under N_2 atmosphere with a 100 W tungsten lamp for 1 week. The formation of **Mt** was followed by IR spectra observing the CO stretching band (ν_{CO} = 1963 cm^{-1} in *n*-hexane). The reaction reached equilibrium after 1 week and, under these conditions, the concentration of **Mt** was 40%. The powdered solid was dissolved in *n*-hexane, filtered, cooled to 0 °C and saturated with CO. The complex **Mc** reacted to give **At**, which was crystallized at −18 °C; in the meantime, the solution concentrated into the complex **Mt**, which, at this temperature, did not react with CO. Repeating this procedure twice, the concentration of **Mt** reached 90%. Further concentration of **Mt** was not possible, so the solid was crystallized from this solution and used for the kinetic measurements. **Mt** was characterized spectroscopically by comparing it with the analogous iron complex [10]: IR spectrum (*n*-hexane): ν_{CO} = 1963 (vs), 2020 (vw) cm^{-1}; ^1H NMR spectrum (CD_2Cl_2): δ_{CH_3} = −0.23 (t) ppm, $^3J_{HP}$ = 5.3 Hz; δ_{PMe_3} = 1.63 (t) ppm, $|^2J_{PH} + {}^4J_{PH}|$ = 3.6 Hz; ^{31}P NMR spectrum (CD_2Cl_2): δ_P = −11.8 (s) ppm.

2.4. Equilibrium constants

Measurements of equilibrium constants were performed in toluene. The experimental procedure for the preparation of CO–N_2 mixtures and measurements of CO concentrations were similar to those described in Ref. [8]. In a typical experiment 10 ml of a solution of **Mc** in toluene ($(1–2) \times 10^{-3}$ M) was introduced into a thermostatted reactor filled with the gas mixture. When the reaction was at equilibrium, the IR spectrum was recorded in the CO stretching region. The concentrations of **Mc** and **At** were determined by Beer's law. This was obtained, for **At**, by preparing standard solutions in CO atmosphere in order to avoid the transformation of **At** into **Mc**: at P_{CO} = 1 atm, appreciable concentrations of **Ac** and **Mc** were present at equilibrium, but the slow rate of reaching equilibrium allowed the **At** concentration to be measured. The concentration of **Ac** was calculated by taking the difference between the initial concentration of **Mc** and the equilibrium concentration of **Mc** and **At**. The equilibrium conditions were also obtained by starting from complex **At**. The equilibrium constants, so obtained, were within the same limits of experimental errors.

2.5. Kinetic measurements

In all the measurements, the carbon monoxide concentrations were much greater than the complex (ratio 10:1), using a thermostatted reactor of 300 ml.

(a) The rate of formation of **At** (Scheme 1) in toluene with varied CO pressures (0.1–0.5 atm) and temperatures (4.7–15 °C) was followed. During each kinetic run the CO pressure was held constant. IR spectroscopy was

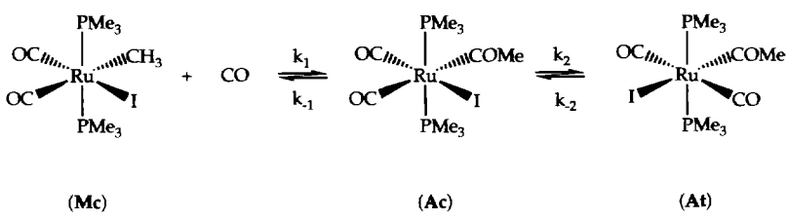

(Mc) (Ac) (At)

Scheme 1.

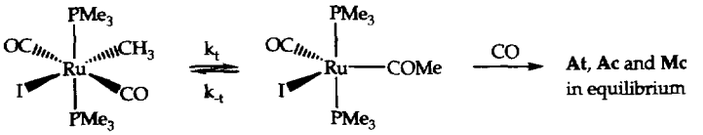

(Mt)

Scheme 2.

used to determine the concentration of complexes. The concentration of **Mc** was followed by the disappearance of both the CO stretching modes (2015, 1955 cm^{-1}); the concentration of **Ac** was obtained by following the CO stretching mode at 2035 cm^{-1}. The concentration of **At** was not followed directly due to the partial superimposition of the CO stretching mode (1983 cm^{-1}) with that of **Ac** (1974 cm^{-1}). The **Mc**, **Ac** and **At** were in equilibrium after carbonylation in the investigated temperature and pressure ranges.

The pseudo-first-order rate constants were obtained from

$$\ln\left(\frac{D_o - D_e}{D_t - D_e}\right) = (k_{fwd} + k_{rev})t = k_{fwd}\frac{a}{x_e}t \qquad (1)$$

where D_o, D_e and D_t were absorbances of complex **Mc** or **At** at zero, equilibrium and time t, k_{fwd} and k_{rev} were the pseudo-first-order rate constants for the forward and the reverse reactions respectively, and a and x_e were the initial and the equilibrium concentrations of **Mc** and **At** respectively.

(b) The decarbonylation of complex **At** was followed in toluene on varying the CO pressure from 0.1 to 0.175 atm in the temperature range 10–20 °C. The pseudo-first-order rate constants were obtained by Eq. (1). The appearance of the CO stretching mode of **Mc** was observed in the IR spectrum at 1955 cm^{-1}. In this case a was the initial concentration of **At** and x_e the equilibrium concentration of **Mc**.

(c) The carbonylation reaction of **Mt** went to completion and was followed in toluene from 0.1 to 1.0 atm of CO pressure in the temperature range 30–50 °C. The reaction rates were lower than those of the **Mc** carbonylations and of the **At** decarbonylation; the reaction products were **Mc**, **At** and **Ac** in equilibrium (Scheme 2). The reaction rate was followed by the disappearance of the CO stretching mode at ν_{CO} = 1963 cm^{-1} of **Mt** and the pseudo-first-order rate constant was calculated from

$$\ln\frac{D_o}{D_t} = k_{obs}t \qquad (2)$$

where D_o and D_t were respectively the absorbances at zero and t times of the CO stretching mode of **Mt** at 1963 cm^{-1}.

3. Results

3.1. Photochemical isomerization of Mc

Complex **Mt** was prepared by photochemical isomerization of **Mc** in the solid state, which is slower than that of the isoelectronic iron complex. The equilibrium concentration of **Mt** is 40%, while it can be as high as 80% for the iron complex [9]. Attempts to prepare **Mt** by photochemical isomerization in solution afford decomposition products and **At**.

The mechanism of the thermal and photochemical isomerization of $[M(CO)_2L_2X_2]$ complexes (M = Ru [16], Fe [17]; L = phosphine ligands; X = halides) has been extensively studied in solution. It proceeds via phosphine or carbon monoxide dissociation. In contrast, the photochemical isomerization in the solid state of the ruthenium complex **Mc** can proceed with the formation of an excited state, in which the ionization of the Ru–I is easy and the rearrangement to the **Mt** structure is possible, as previously hypothesized for isoelectronic complexes of iron [8]. The energy barrier of this rearrangement for the iron complex has been estimated to be less than 10–12 kJ [18]; it can also occur in the solid state.

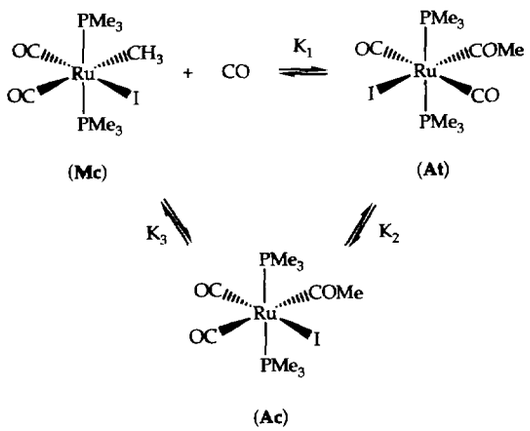

(Mc) (At)

(Ac)

Scheme 3.

Table 1
Equilibrium constants at various temperatures for the reactions of Scheme 1 in toluene

T (°C)	$10^{-2}K_1$ (M^{-1})	$10^{-1}K_3$ (M^{-1})
24.5	17.39	18.94
	18.97	14.22
33.8	12.22	11.38
42.0	6.94	8.49
	6.59	8.67
49.3	4.06	4.88
56.5	2.90	3.15
64.4	1.96	2.10
74.3	1.20	1.65

It was not possible to obtain pure **Mt**; therefore, it was only characterized spectroscopically. The IR spectrum shows two CO stretching modes at 2020(vw) and 1963(vs) cm^{-1} (*n*-hexane) in agreement with two CO ligands in the trans position; the ^1H NMR spectrum in CD_2Cl_2 shows a 'deceptive' triplet [19] indicating that the two PMe_3 ligands are magnetically equivalent. Having fixed the two CO in the relative trans position, the two phosphines must have a relative trans position too. The remaining CH_3 and iodide ligands must be in the relative trans position.

3.2. Thermodynamic and kinetic results

The equilibrium constants in toluene at various temperatures and CO pressures, which refer to the reactions reported in Scheme 3, are reported in Table 1. K_2 equilibrium constants are not shown in Table 1 because they depend on K_1 and K_3 (the analytical concentration of **Ac** was not measured directly, see Section 2.4).

The pseudo-first-order rate constants of the carbonylation of complex **Mc** and of the decarbonylation of complex **At** in toluene at various temperatures and CO pressures are given in Tables 2 and 3 respectively.

A summary of the rate constants of the carbonylation and decarbonylation reactions and the thermodynamic and kinetic parameters are given in Table 4.

The pseudo-first-order rate constants of the carbonylation of **Mt** in toluene at various temperatures and CO pressures are given in Table 5.

Table 2
Pseudo-first-order rate constants [a] k_{fwd} in toluene for the carbonylation reaction of **Mc**

T (°C)	P_{CO} (atm)	10^3[CO] (M)	10^4k_{fwd} (s^{-1})
4.7	0.50	4.26	7.77(0.33)
	0.25	2.13	6.83(0.17)
	0.175	1.49	5.84(0.33)
	0.125	1.06	4.92(0.07)
	0.10	0.85	4.18(0.14)
9.7	0.50	4.01	13.51(0.73)
	0.25	2.00	11.16(0.42)
	0.175	1.40	10.22(0.51)
	0.125	1.00	7.53(0.21)
	0.10	0.80	6.98(0.22)
15.0	0.375	2.89	24.67(0.13)
	0.25	1.88	22.86(0.66)
	0.175	1.32	17.84(0.29)
	0.125	0.94	10.87(0.15)
	0.10	0.75	10.13(0.27)

[a] The values in parentheses are the standard deviations of four measurements.

Table 3
First-order rate constants k_{fwd} for the decarbonylation reaction of **At** in toluene at various temperatures

T (°C)	10^2P_{CO} (atm)	10^4k_{fwd} (s^{-1})
10.0	4.0	2.18
	3.5	2.18
	2.5	2.37
	1.75	2.42
15.0	10.0	4.32
	4.0	4.74
	2.5	4.56
20.0	10.0	9.64
	4.0	10.80
	2.5	11.60

Table 4
Summary of k_2, k_1/k_{-1}, k_{-2}, thermodynamic and activation parameters [a] for the carbonylation reaction of **Mc** and decarbonylation reaction of **At**

T (°C)	10^3k_2 (s^{-1})	k_1/k_{-1} (M^{-1})	10^4k_{-2} (s^{-1})
4.7	1.04(0.20)	813	
9.7	2.02(0.38)	641	
15.0	4.77	348	4.54(0.21)
10.0			2.29(0.13)
20.0			10.68(0.99)

Thermodynamic and activation parameters:

$\Delta H^{\#}(k_2) = 102(2)$ kJ mol^{-1} $\Delta S^{\#}(k_2) = 67(7)$ J K^{-1} mol^{-1}

$\Delta H(k_1/k_{-1}) = -52(14)$ kJ mol^{-1} $\Delta S(k_1/k_{-1}) = -113(50)$ J K^{-1} mol^{-1}

$\Delta H^{\#}(k_1k_2/k_{-1}) = 43(7)$ kJ mol^{-1} $\Delta S^{\#}(k_1k_2/k_{-1}) = -83(23)$ J K^{-1} mol^{-1}

$\Delta H^{\#}(k_{-2}) = 105(5)$ kJ mol^{-1} $\Delta S^{\#}(k_{-2}) = 57(14)$ J K^{-1} mol^{-1}

[a] Values in parentheses are the standard deviations at the 95% confidence limit.

Table 5
Pseudo-first-order rate constants [a] k_{obs} in toluene for the carbonylation reaction of **Mt** at various temperatures

T (°C)	P_{CO} (atm)	10^6k_{obs} (s^{-1})
30.0	0.2	5.68(0.32)
	1.0	5.56(0.30)
40.0	0.1	26.9(0.55)
	0.2	26.0(0.62)
	1.0	28.7(0.75)
50.0	0.1	84.8(0.82)
	0.2	89.0(0.75)
	1.0	79.0(1.20)

[a] Values in parentheses are the standard deviations of four measurements.

Table 6
Comparison of rate constants, thermodynamic and activation parameters for the carbonylation and decarbonylation reactions of ruthenium and iron complexes in toluene at 20 °C [a]

	Fe	Ru
K_1 (M^{-1})	73000	2582
ΔH_1 (kJ mol^{-1})	−60(4)	−47.5(3)
ΔS_1 (J K^{-1} mol^{-1})	−111(8)	−97(9)
K_2	31	11.8
ΔH_2 (kJ mol^{-1})	−18(4)	−6(6)
ΔS_2 (J K^{-1} mol^{-1})	−33(12)	0(20)
K_3 (M^{-1})	1454	231
ΔH_3 (kJ mol^{-1})	−47(4)	−42(6.5)
ΔS_3 (J K^{-1} mol^{-1})	−100(12)	−98(21)
k_2 (s^{-1})	7.65×10^{-4}	9.75×10^{-3}
$\Delta H_2^{\#}$ (kJ mol^{-1})	95(4)	102(2)
$\Delta S_2^{\#}$ (J K^{-1} mol^{-1})	20(5)	67(7)
k_{-2} (s^{-1})	7.62×10^{-6}	10.7×10^{-4}
$\Delta H_{-2}^{\#}$ (kJ mol^{-1})	86(7)	105(5)
$\Delta S_{-2}^{\#}$ (J K^{-1} mol^{-1})	−36(25)	57(14)
k_t (s^{-1})	2.50×10^{-7}	1.31×10^{-6}
$\Delta H_t^{\#}$ (kJ mol^{-1})	110(4)	105(10)
$\Delta S_t^{\#}$ (J K^{-1} mol^{-1})	4(12)	3(13)

[a] Values in parentheses are the standard deviations at the 95% confidence limits.

A comparison of rate constants, thermodynamic and activation parameters of the carbonylation and decarbonylation reactions of ruthenium and iron complexes in toluene at 20 °C are given in Table 6.

4. Discussion

4.1. Thermodynamic results

Both the carbonylation reaction of **Mc** to **At** and **Ac** are exothermic ($\Delta H_1 = -47.5(3)$ kJ mol^{-1}; $\Delta H_3 = -42(6.5)$ kJ mol^{-1}). Due to the large loss of rotational and translational entropy by CO(g) upon insertion [20], the negative carbonylation entropy values are nearly the same in both two reactions ($\Delta S_1 = -97(9)$ J K^{-1} mol^{-1}; $\Delta S_3 = -98(21)$ J K^{-1} mol^{-1}). The greater stability of **At** with respect to **Ac** is essentially caused by the enthalpic term influenced by the steric hindrance of I.

A comparison of these values with the corresponding ones of the iron complexes (Table 6) indicates that acetyl complexes of iron are more stable than the ruthenium ones ($K_1 = 73\,000$ M^{-1} for iron and 2580 M^{-1} for ruthenium; $K_3 = 1454$ M^{-1} for iron and 231 M^{-1} for ruthenium at 20 °C). This is a general trend for metals of the same group with increasing period. The acetyl complex is more stable with respect to the methyl ones for metals of the second and third periods and is due to the increasing strength of the M–R bond [21].

A comparison of the isomerization equilibria ($K_2 =$ 31 for iron and 11.8 for ruthenium) suggests that **At** is more stable with iron than with ruthenium, in agreement with the prevalent influence of the steric effect which is greater in the more crowded iron complexes [22].

4.2. Reaction mechanism

4.2.1. Carbonylation of Mc

The carbonylation process in toluene is represented in Scheme 1. The first step (**Mc–Ac**) is very fast and is experimentally impossible to follow by conventional techniques. During this step, **Ac** forms from **Mc** until equilibrium is reached. Subsequently, **Ac** isomerizes to **At**, while the **[Ac]/[Mc]** ratio remains constant and reaches a final equilibrium with **At**. The kinetics were followed during the attainment of equilibrium with **At** and treated according to Scheme 1 where the first step is much faster than the second. This allows **Mc** and **Ac** to be at equilibrium during the formation of **At** [23].

On the basis of the mass conservation law and equilibrium requirements [24] and assuming that $k_2 \ll k_{-1}$, the first-order rate constants k_{fwd} follow Eq. (3):

$$k_{fwd} = \frac{k_1 k_2 [CO]}{k_1 [CO] + k_{-1}} \quad (3)$$

The assumption that $k_2 \ll k_{-1}$ seems to be reasonable owing to the fast attainment of the **Mc–Ac** equilibrium compared to that of **Ac** and **At**.

Rearrangement of Eq. (3) yields

$$\frac{1}{k_{fwd}} = \frac{1}{k_2} + \frac{k_{-1}}{k_1 k_2 [CO]} \quad (4)$$

Plots of $1/k_{fwd}$ vs. $1/[CO]$ give a straight line with $1/k_2$ as intercept and $k_{-1}/k_1 k_2$ as slope (Fig. 1). The values of k_2 and k_1/k_{-1} at various temperatures are given in Table 4. Within the limits of the experimental

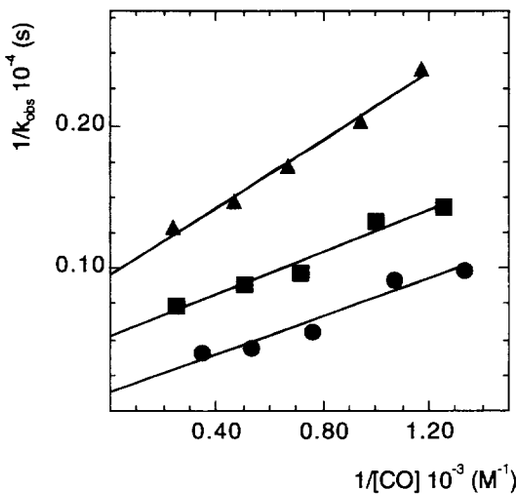

Fig. 1. Plots of $1/k_{fwd}$ vs. $1/[CO]$ at various temperatures in toluene: (▲) $T = 4.7$ °C; (■) $T = 9.7$ °C; (●) $T = 15$ °C.

error, k_1/k_{-1} values are in agreement with the experimental equilibrium K_3 constants (see Section 4.1).

The rate constants of the isomerization step (k_2) are independent of the CO concentration; therefore, the positive effect of the CO pressure on the rate of the isomerization reaction, reported in the literature [12,20], can only be explained as a shift of the carbonylation equilibrium towards the **Ac** complex.

The decarbonylation reaction of **At** follows a first-order kinetic law (Table 3) and, since the decarbonylation of **Ac** is much faster than the isomerization reaction, the total reaction rate is determined by this last process ($k_{rev} = k_{-2}$).

A comparison of the kinetic results of the isomerization reaction of ruthenium and iron shows that ruthenium has a higher reactivity. The rate constant ratios $k_2(Ru)/k_2(Fe)$ and $k_{-2}(Ru)/k_{-2}(Fe)$ are 12 and 140 respectively and are not due to the activation enthalpy, which is lower for iron (Table 6), but rather to the entropic term.

Neither the carbonylation nor decarbonylation kinetic results provide information on the mechanism of the insertion step of Scheme 1. However labelling experiments with ^{13}CO [11] exclude the formation of labelled $^{13}COMe$, in moderately polar solvents, as observed for the iron isoelectronic complexes [25], and therefore exclude the ionization of the Ru–I bond in **Mc** at least in these solvents. This supports the methyl migration mechanism, previously proposed by Mawby and coworkers [10] that proceeds with the formation of an unsaturated pentacoordinated intermediate which rearranges and reacts with CO to give **Ac** and **At** complexes. Since the CO concentration influences both the formation of **Ac** and **At**, the isomerization reaction is not influenced by the CO concentration in agreement with the experimental results.

The activation parameters for the formation of **At** from **Mc** can be calculated for iron and ruthenium complexes. The values are $\Delta H^{\#} = 47\,kJ\,mol^{-1}$ and $\Delta S^{\#} = -91\,J\,K^{-1}\,mol^{-1}$ for iron and $\Delta H^{\#} = 54.5\,kJ\,mol^{-1}$ and $\Delta S^{\#} = -30\,J\,K^{-1}\,mol^{-1}$ for ruthenium. These values are in agreement with the $M–CH_3$ bond strength, which is lower for the iron complexes with respect to the isoelectronic ruthenium complexes [26]. In general, the difference in the M–R bond strength between the metals of the first and second transition series is ca. $15–20\,kJ\,mol^{-1}$.

4.2.2. Carbonylation of Mt

Complex **Mt** reacts with CO to give an equilibrium mixture of **At**, **Ac** and **Mc**. The pseudo-first-order rate constants reported in Table 5, within the limits of the experimental error, are independent of the CO pressure. This suggests that the carbonylation mechanism proceeds via methyl migration with the formation of an unsaturated pentacoordinated intermediate $Ru(CO)(PMe_3)_2(COMe)I$ which rearranges to give **Ac**, **At** and **Mc** (Scheme 2).

The pseudo-first-order rate constants k_{obs} correspond to the first order rate constants k_t of the migration step (Scheme 2). The k_t values are higher than the corresponding iron values (Table 6). No appreciable differences in the activation enthalpy and entropy are observed.

The lower reactivity of the iron **Mt** complex can be explained on the basis of its higher stabilization due to the steric hindrance of I which is more effective in the iron complexes than in the ruthenium ones as observed in the **Ac** and **At** complexes.

The reaction rate of **Mt** is much lower than **Mc**: the ratio between the half-life times of these two reactions are $< 10^{-5}$. This can be explained on the basis of the effect of the methyl trans ligand as proposed by Berke and Hoffmann [27] and observed experimentally by Kubota et al. [28].

5. Conclusions

Both **Mc** and **Mt** complexes of ruthenium react with carbon monoxide via the methyl migration mechanism; the **Mt** iron complex also reacts with this mechanism, while the **Mc** reacts via the ionization mechanism. The ruthenium complexes are more reactive than the iron ones, while the $M–CH_3$ bond strength is stronger for ruthenium. The acetyl **Ac** and **At** complexes are relatively more stable than the methyl **Mc** ones for iron, in agreement with the lower $Fe–CH_3$ bond strength.

Acknowledgements

This work was supported by grants from the Consiglio Nazionale delle Ricerche (CNR, Roma, Italy) and the Ministero dell'Università e della Ricerca Scientifica e Tecnologica (MURST, Roma, Italy). The authors would like to thank Francesco Spano for technical assistance.

References

[1] J. Tsuji, Organic Syntheses by Means of Transition Metal Complexes, Springer, Berlin, 1975.
[2] F. Calderazzo, Angew. Chem. Int. Ed. Engl. 16 (1977) 299–311.
[3] A. Wojcicki, Adv. Organomet. Chem. 11 (1973) 87–145.
[4] J.J. Alexander, in: F.R. Hartley, S. Patai (Eds.), The Chemistry of Metal–Carbon Bond, vol. II, Wiley, 1985, pp. 339–400.
[5] K. Noack, F. Calderazzo, J. Organomet. Chem. 10 (1967) 101–104.
[6] J.N. Cause, R.A. Fiato, R.L. Pruett, J. Organomet. Chem. 172 (1979) 405.
[7] M. Bassetti, D. Monti, A. Haynes, J. Pearson, I. Stanbridge, P.M. Maitlis, Gazz. Chim. It. (1992) 391–393. P.M. Maitlis, A.

Haynes, G.J. Sunley, M.J. Howard, J. Chem. Soc. Dalton Trans. (1996) 2187–2196.
[8] G. Bellachioma, G. Cardaci, C. Jablonski, A. Macchioni, G. Reichenbach, Inorg. Chem. 32 (1993) 2404–2409.
[9] G. Bellachioma, G. Cardaci, A. Macchioni, G. Reichenbach, E. Foresti, P. Sabatino, J. Organomet. Chem. 531 (1997) 225–233.
[10] C.F.J. Barnard, J.A. Daniels, R.J. Mawby, J. Chem. Soc. Dalton Trans. (1979) 1331–1338. C.F.J. Barnard, J.A. Daniels, R.J. Mawby, J. Chem. Soc. Chem. Commun., (1976) 1032.
[11] G. Cardaci, G. Reichenbach, G. Bellachioma, B. Wassink, M.C. Baird, Organometallics 7 (1988) 2475–2479.
[12] (a) M. Pankowski, M. Bigorgne, M. VIII ICOC, 1977, Kyoto, Japan. (b) M. Pankowski, M. Bigorgne, J. Organomet. Chem. 251 (1983) 333–338.
[13] A. Wolfsberger, H. Schmidbaur, Synth. React. Inorg. Met. Org. Chem. 4 (1974) 149–154.
[14] G. Cardaci, J. Organomet. Chem. 323 (1987) C10–C12.
[15] A. Weissberger, E.S. Proskauer, Technique of Organic Chemistry, vol. III, Interscience, New York, 1955.
[16] D.W. Krassowski, J.M. Nelson, K.R. Brower, D. Hauerstein, R.A. Jacobson, Inorg. Chem. 27 (1988) 4294–4307.
[17] M. Pankowski, M. Bigorgne, J. Organomet. Chem. 125 (1977) 231–252. M. Pankowski, M. Bigorgne, J. Organomet. Chem. 19 (1969) 393–398.
[18] G. Reichenbach, personal communication.
[19] R.K. Harris, Can. J. Chem. 42 (1964) 2275.
[20] J.A. Connor, M.T. Zafarani-Moattar, J.B. Bickerton, N.I. El Sayed, S. Suradi, R. Carson, G. Al Takhin, H.A. Skinner, Organometallics 1 (1982) 1166–1174.
[21] E.J. Kuhlmann, J.J. Alexander, Coord. Chem. Rev. 33 (1980) 195–225.
[22] G. Reichenbach, G. Cardaci, G. Bellachioma, J. Chem. Soc. Dalton Trans. (1982) 847.
[23] R.G. Wilkins, Kinetics and Mechanism of Reactions of Transition Metal Complexes, VCH, Weinheim, 2nd edition, 1991, pp. 33–37.
[24] D. McDaniels, C.R. Smoot, J. Phys. Chem. 60 (1956) 966–969.
[25] G. Cardaci, G. Reichenbach, G. Bellachioma, Inorg. Chem. 23 (1984) 2936–2940.
[26] C. Mancuso, J. Halpern, J. Organomet. Chem. 428 (1992) C8–C11. J. Halpern, Acc. Chem. Res. 15 (1982) 238–244.
[27] H. Berke, R. Hoffmann, J. Am. Chem. Soc. 100 (1978) 7224–7236.
[28] M. Kubota, T.M. Mc Clersky, R.K. Hayashi, G. Webb, J. Am. Chem. Soc. 109 (1987) 7569–7570.